ACS APPLIED MATERIALS & INTERFACES

Research Article

www.acsami.org

Photopatternable Electrochromic Materials from Oxetane Precursors

Antoine Leliège, Satyananda Barik,[†] and W. G. Skene*

Laboratoire de caractérisation photophysique des matériaux conjugués, Département de Chimie, Pavillon JA Bombardier, Université de Montréal, CP 6128, succ. Centre-ville, Montréal, Québec, Canada H3C 3J7

Supporting Information

ABSTRACT: Conjugated thiophenoazomethine triads containing an acid sensitive oxetane group were prepared. The solution processable monomers were immobilized on glass and ITO coated glass substrates by photoacid induced cationic ring-opening polymerization (CROP) of the oxetane moiety. Photolithography using a photoacid generator and photosensitizer were used to pattern an electroactive polymer. Micro- and macroscale patterns ranging between 20 μm and 50 mm were possible with the electrochromic materials. The photopolymerized azomethine remained electroactive, and it could be repeatedly switched electrochemically between its neutral (mauve, λ_{max} = 535 nm) and oxidized (blue, λ_{max} = 585 nm) states without degradation. The electrochromic properties were evaluated in a simulated device where the colors were successfully cycled between blue (oxidized) and purple (neutral) states with applied biases of +0.6 V and −0.6 V vs Fc/Fc$^+$ under ambient conditions without significant color fatigue or degradation.

KEYWORDS: *Photolithographic patterning, cationic ring-opening polymerization, electroactive polymers*

INTRODUCTION

Functional materials capable of color switching between different states are of interest to meet the ever changing demands of consumer electronics.[1−3] Thiophene based polymers have found uses in certain electrochromic devices as a result of intrinsic contrasting colors between the neutral and oxidized forms concomitant with forming stable intermediates.[4−7] As the need for a wider range of color states for consumer electronics has grown, interest in contemporary thiophene polymers has waned and the search for novel electrochromic materials has intensified.[8,9]

Improved electrochromic properties have recently been achieved by incorporating vinylene linkages, which promote coplanarization and extended conjugation within the polythiophene backbone.[10,11] Moreover, vinylene linkages have allowed insertion of electron donating and/or accepting groups into the polymer.[10,12,13] The preparation of these derivatives requires rigorous reaction conditions such as anhydrous solvents and inert atmospheres. Furthermore, such coupling methods produce significant byproducts that require tedious product purification for obtaining pristine materials and for ensuring optimal color and device performance. The preparation of electrochromic materials derived from vinylenes is complicated because solubility must be designed into the resulting polymers to make them processable for device preparation.[14−19]

While polymer solubility in organic solvents is important for coating usage and device preparation, it is problematic for electrochromic devices.[20,21] This is because solution processable polymers often dewet from the electrode.[6,19,22] The polymer subsequently mixes unwantedly with the required electrolyte ion conducting gel. This leads to localized short-circuiting and ultimate device malfunctioning. The collective challenges limit the device longevity and dilute the color transitions between the *on*/*off* states. Recently, the delamination problem has been in part addressed by using polymers whose solubility can be switched thermally or externally via chemical switches.[23−30] An alternative approach is the thermal or electrochemical polymerization of monomers directly on device electrodes.[31−35]

Immobilization of conjugated materials using oxetane derivatives is a viable alternative to other immobilization strategies. Oxetanes undergo cationic ring-opening polymerization (CROP) to form insoluble polyethers (Supporting Information Scheme S1).[36−39] An advantage of oxetanes is they can be easily incorporated into small molecules. These can then be immobilized directly on substrates, precluding the need for solution processable polymer precursors for subsequent immobilization using external triggers. More importantly, CROP of oxetane derivatives can selectively be done photolithographically. With the use of photoacid generators, CROP results in well-defined patterns of high resolution and variable dimensions that can even potentially be scaled-down to nanometer resolution.[40] Despite the advantages of oxetanes, they have never been applied for immobilizing electroactive layers in plastic devices, especially electrochromic devices.

Conjugated azomethines are proven alternatives to their vinylenes counterparts, in part due to the isoelectronic character with their all-carbon counterparts.[41,42] Azomethines are, however, believed to be hydrolytically and anodically

Received: February 3, 2014
Accepted: April 10, 2014
Published: April 10, 2014

   dx.doi.org/10.1021/am500726n | ACS Appl. Mater. Interfaces 2014, 6, 6920−6929

Scheme 1. Synthetic Scheme for the Preparation of the Azomethine Oxetane Derivative 5[a]

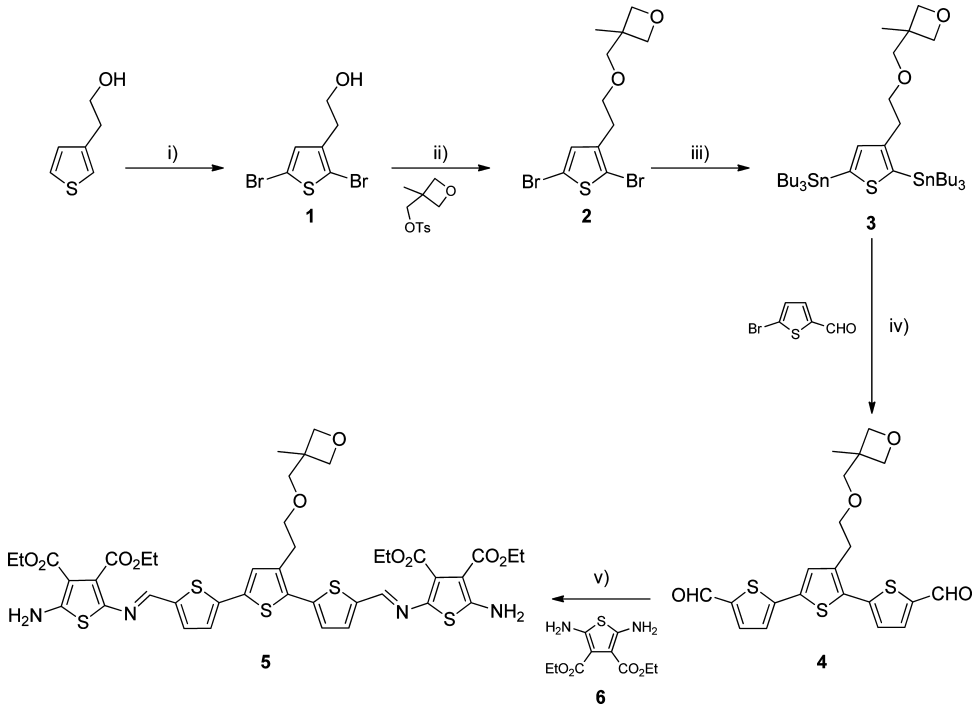

[a](i) NBS, DMF 93%; (ii) KOH, THF, 72%; (iii) (a) *n*-BuLi, (b) Bu_3SnCl, THF; (iv) $Pd(PPh_3)_4$, toluene 47%; (v) $Sc(SO_3CF_3)_3$, EtOH, 76%.

unstable and thought ill-suited for applications as electrochromic materials. This is in part because of their poor properties such as irreversible oxidation and high oxidation potentials. We recently disproved this by demonstrating that highly conjugated azomethines having properties suitable for electrochromic device use are possible.[43,44] To further demonstrate the robustness of the conjugated azomethines for electrochromic devices, especially for preparing immobilized electroactive polymers having discrete patterns, we prepared and investigated the photopatterning of the oxetane azomethine derivative **5** (Scheme 1). This is of particular importance given the acidic conditions of photolithographic CROP are generally assumed to hydrolyze the azomethine and destroy its inherent electrochromic properties. More importantly, CROP of oxetane derivatives has not been previously used to fabricate electrochromic devices. Rather, this method of active layer immobilization is in its infancy, and it has been exclusively used for OLED device fabrication and only recently has been extended to photovoltaic applications.[37−39,45−48] Given this technology has not been exploited for electrochromic applications and especially not with azomethines, the photolithography of **5** was therefore proven by patterning immobilized electrochromic layers directly on the device electrodes. The electrochromic properties of the photopatterned layer were investigated to demonstrate that small molecules of conjugated azomethines can be successfully immobilized while preserving their electroactivity. This proof-of-principle study is of importance for proving that both azomethines and CROP are viable alternatives to current electrochromes for preparing photopatterned electroactive layers.[49−51] The mutual suitability of azomethines and their immobilization by photoinduced CROP for use in electrochromic devices are herein demonstrated.

RESULTS AND DISCUSSION

Synthesis. The conjugated azomethine **5** was targeted because it was expected to possess the properties desired for its eventual use in electrochromic devices. A key property anticipated with **5** was reversible oxidation owing to the amines in the terminal positions that prevent the electrochemically generated radical cation from reacting via standard anodic polymerization.[52] For use in electrochromic devices, especially display and sign applications, intense absorbance of both the neutral and oxidized states in the visible portion of the spectrum are beneficial.[53] **5** was expected to possess these optical properties because of its inherent *push−pull* electronic effect courtesy of the conjugated amine−azomethine that results in a strong intramolecular charge transfer. Meanwhile, the acid sensitive oxetane could undergo CROP and convert **5** into a photopolymerized azomethine film that would be immobilized on the working electrode. The photopolymerized film was expected to be insoluble as desired owing to the absence of solubilizing alkyl pendant chains that are typically required for polymer solubility. The oxetane moiety of **5** could also be potentially patterned using standard photolithographic methods.[54]

The synthesis of the targeted **5** was done according to Scheme 1. Bromination of 3-thiophene ethanol with NBS gave **1**. The isolated alcohol was converted into the alkoxide with KOH in ethanol. The intermediate was used as the nucleophile to afford **2** via nucleophilic substitution with 3-methyl-3-(toluene sulfonyloxymethyl) oxetane.[78] The dibromide was converted into the distannyl derivative **3** by reacting **2** with *n*-BuLi at low temperature followed by addition of Bu_3SnCl. Stille coupling between **3**, which was used as is without additional purification, and 5-bromo-2-thiophene carboxaldehyde using a palladium catalyst gave **4** in an overall 47% yield. Condensing **4** with the diaminothiophene **6** was done with scandium

triflate,[35,55,56] instead of typically used trifluoroacetic acid. The latter was thought to preferentially promote CROP of the oxetane moiety, rather than desired imination. The targeted **5** was obtained in 76% yield using the scandium catalyst with minimal undesired CROP of the oxetane moiety.

The photopolymerization of **5** was done using *p*-octyloxyphenyl-phenyl iodonium hexafluoroantimonate (OPPI) as the photoacid generator (PAG).[57−59] While catalytic amounts of the PAG are normally required for CROP, a stoichiometric amount was used. This was to ensure a sufficient amount of acid was available to promote CROP and to take into account the potential protonation of the amines and azomethines of **5** by the photochemically generated acid. It should be noted that the reactivity of the amines of **5** are suppressed owing to the withdrawing effects of the neighboring esters and azomethines.[60] The cyclic ether was therefore expected to be a better nucleophile for promoting CROP among the reagents used. Giving that **5** (λ_{abs} = 492 nm in dichloromethane) strongly absorbs in the visible, it would be an ideal intrinsic photosensitizer for acid generation with the typically used iodonium salt via energy transfer. However, no photoinduced acid CROP was observed by directly irradiating **5** at 350 nm in the presence of OPPI. This was qualitatively determined by the absence of immobilized film on the substrate even after prolonged irradiation times. Instead, the deposited film was dissolved from the substrate upon washing with common organic solvents. To some extent this was not surprising since the azomethine bond is known to efficiently deactivate the singlet state.[61] Oligothiophenes, including terthiophenes, are further known to undergo efficient intersystem crossing.[62−64] The collective deactivation modes are assumed to quench the excited state of **5** before energy transfer to the PAG can occur. A fluorenone derivative was then used as a photosensitizer for energy transfer to the PAG upon irradiation. An anthracene derivative was also used as an accelerator to improve the polymerization time and sensitivity. A photoactive solution consisting of photosensitizer/PAG/accelerator/**5** in a 2:1:1.2:1.6 weight ratio was prepared and coated onto substrates by drop- and spray-coating. A mask with a given pattern was placed over the deposited red films, and they were irradiated at 350 nm for 10 min. The irradiated film was then baked at 100 °C for 60 min to ensure acid diffusion through the films and allow the oxetane moieties to reorganize for maximum CROP.[54,65] The substrates were then rinsed with a mixture of dichloromethane/triethylamine (8/2 vol %) followed by neat dichloromethane. This was necessary to develop the desired image by removing the unexposed **5** that remained soluble.

Azomethines are generally understood to be hydrolytically unstable, especially under the conditions used to promote CROP. Given the significant spectral differences between **4** and **5** (Figure 1), the hydrolysis of **5** to **4** could potentially be tracked spectroscopically. Both absorbance and ATR-FTIR spectroscopies were used to provide additional evidence for the robustness of the azomethine bond toward photopolymerization by CROP. As seen in Figure 1, the absorbance of **5** is bathochromically shifted by ca. 100 nm relative to **4** (Figure 1). This is owing to its increased degree of conjugation and electronic *push*−*pull* effect of the azomethine bond and the terminal electron donating amines. The absorbance of **5** is further red-shifted by ca. 250 nm upon photoinduced CROP. This bathochromic shift is a halochromic effect from protonation of both the terminal amines and azomethines by

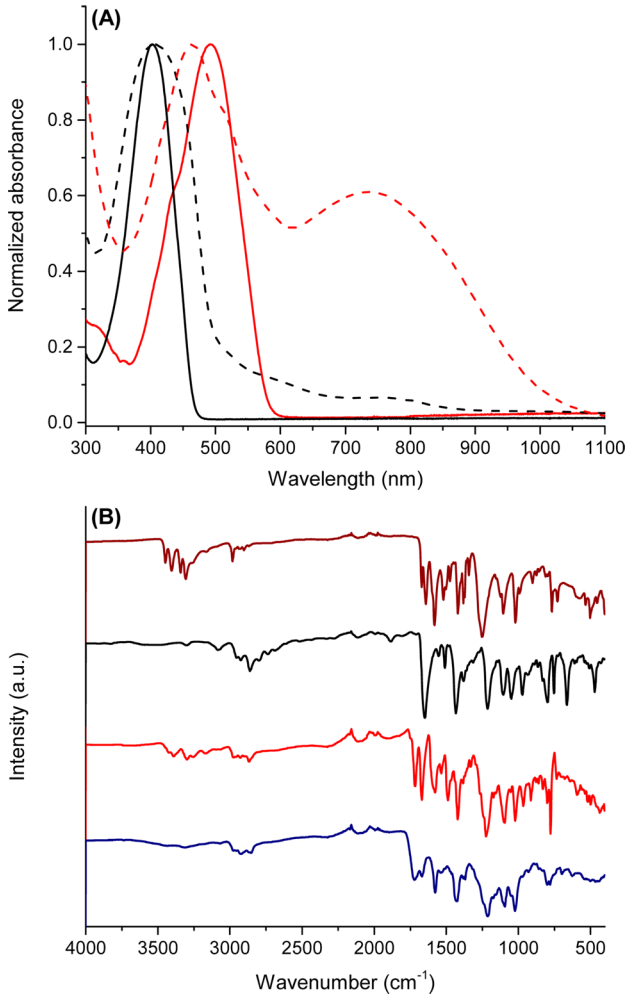

Figure 1. (A) Normalized absorbance spectra of **4** (black solid line) and **5** (red solid line) in dichloromethane along with **4** (black dashed line) and **5** (red dashed line) immobilized on glass by photoinduced CROP prior to rinsing the substrates postpolymerization. (B) ATR-FTIR spectra of **4** (black), **5** (red), **5** immobilized on the surface via CROP (navy), and **6** (wine).

the stoichiometrically photogenerated acid. This was confirmed by the absence of similar spectral shifts when **4** was photopolymerized using the same conditions as **5**. Meanwhile, the weak shoulder at 470 nm corresponds to the photosensitizer (Supporting Information Figure S3) that is removed upon rinsing the substrate postpolymerization. The substrates of **5** were washed postirradiation with dichloromethane solutions containing triethylamine to neutralize the protonated immobilized polymer in addition to removing the residual photoactive CROP reagents and low molecular weight oligomers. Decomposition of **5** by acid promoted hydrolysis either during CROP or by the postpolymerization washing treatment would give **4** as the product. This would be spectroscopically evident by distinctive absorbance of **4** at 400 nm (Figure 1). Washing the photopolymerized **5** led exclusively to the original spectrum of **5** with no absorbance peak at 400 nm, confirming the robustness of the azomethine bond to photoinduced CROP. The persistently immobilized film on the electrode after repeated rinsing with solvents known to remove **5** further confirmed the polymeric nature of the immobilized layer prepared by CROP. It is noteworthy that monomers generally containing two oxetane moieties are

dx.doi.org/10.1021/am500726n | ACS Appl. Mater. Interfaces 2014, 6, 6920−6929

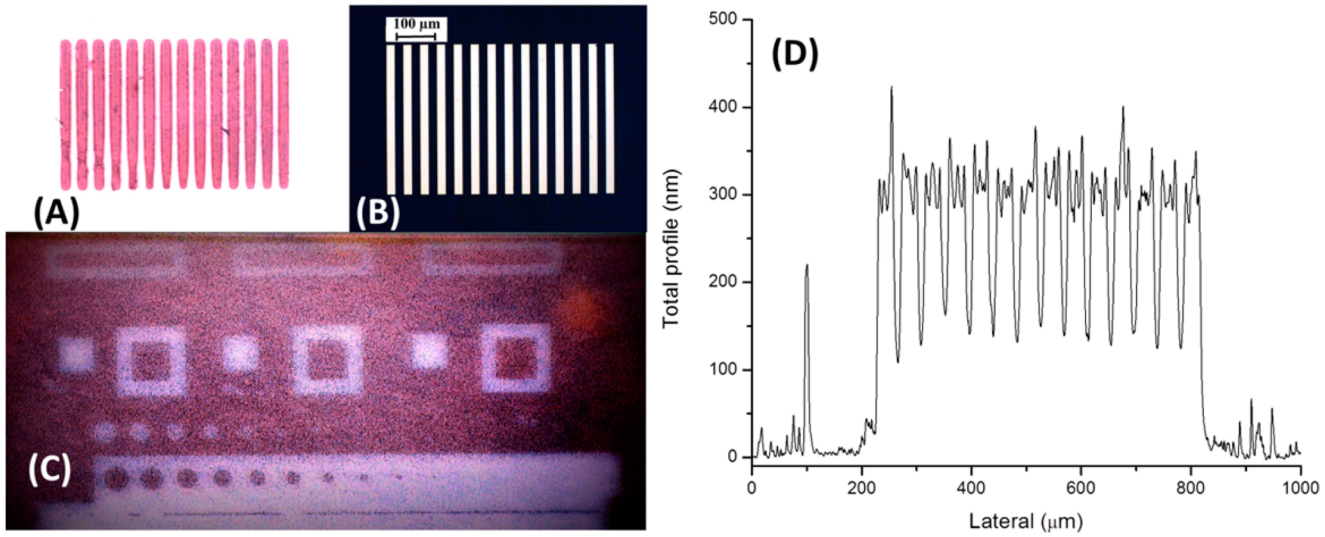

Figure 2. Photographs of the resulting immobilized **5** upon irradiating, curing, and postpolymerization washings (A) taken with an optical microscope and the photomask used for photopatterning (B). Photograph of large area photopatterning of **5** on glass (C) measuring 52 mm in length. The reference length bar shown is 100 μm for (B). Profilometry of photopolymerized **5** on glass (D) after photolithography using the mask from (B).

required to obtain cross-linked immobilized polymer films by CROP.[66] The advantage of the single oxetane containing **5** is it relative synthetic ease compared to analogous bisoxetanes.

CROP of the oxetane moiety and polymer film formation were additionally supported by ATR-FTIR. This was confirmed by the disappearance of the characteristic oxetane peak at ca. 970 cm^{-1} when both **4** and **5** were irradiated with the PAG and photosensitizer.[67] FTIR was also used to confirm the absence of hydrolysis of **5** into **4** during photoinduced CROP. This was done on the basis of the peak at 1649 cm^{-1} that corresponds to the terminal carbonyl of **4** (Supporting Information Figure S7). This peak did not appear in the immobilized films of **5** even at irradiation times longer than those used to produce the photopatterns in Figure 2.

Desired immobilization of **5** via photoacid induced ring-opening polymerization was qualitatively assessed. This was done by analyzing the persistent purple color of the immobilized film on the substrates via optical microscopy (Figure 2A). The color difference of Figures 2A and 2C compared to the insets of Figures 4B and 5B observed for the same sample is uniquely from the color filter used for the optical microscope camera. Therefore, the images of the immobilized **5** taken with the optical microscope are not true representative colors. This withstanding, the films resisted repeated washings, confirming the extended polymerization of **5** upon irradiation. The persistent purple color after postpolymerization washings also confirmed the photopolymerized **5** resisted hydrolysis by the PAG and it does not hydrolyze to **4** during photolithography and curing. Photolithography of **5** using the PAG mixture was also done by both spray-coating and drop-casting solutions. These deposition methods were pursued because the optical contrast of the fine photopatterns obtained by preliminarily investigated films prepared by spin-coating was too low to be evaluated by optical microscopy. What appears as cracks in the image of Figure 2C are actually regions of different thickness of the photopolymerized film. This is a result of inconsistent coating thickness from manual spray-coating of **5**, resulting in a rough layer of deposited material and not from defects in the image transfer. This is supported by the high resolution image produced with thicker films by drop-casting (Figure 2A). Photomasks having 20 μm images were used as a proof-of-concept to demonstrate that **5** could successfully transfer the patterns photolithographically. Photographs of a typical photomask used for patterning and the resulting photopattern obtained by **5** are seen in parts B and A of Figure 2, respectively. Images of different resolutions ranging between 20 μm and upward of 50 mm could be obtained by photopatterning **5** (Figure 2C). Well resolved large-scale images on the centimeter scale could also be obtained (Supporting Information Figures S11 and S12).

The resulting photopatterned images were further quantified by profilometry. Figure 2D shows the ca. 600 μm cross-section of the photopolymerized **5** from image Figure 2A. This image was obtained after exposing a drop-casted film of the PAG mixture with the mask in Figure 2B followed by developing. Image development consisted of thermally curing the substrate postirradiation followed by thorough rinsing with triethylamine solutions diluted in dichloromethane and neat dichloromethane. The image clearly shows that well-resolved 10 μm valleys and 30 μm plateaus were obtained. The width of the plateaus and valleys mimic the photopattern dimensions, confirming that **5** can successfully transfer the image and that an immobilized film can be obtained. The observed design features and high resolution of the transferred image confirm that **5** does not hydrolyze or decompose with the CROP conditions.

A pivotal property required of electrochromic materials is electrochemical reversibility. The electrochemistry of **5** was therefore investigated. Only the anodic properties were probed because thiophenes are known to be exclusively p-type materials.[68,69] As seen in Figure 3, **5** exhibits a reversible oxidation with E_0' = 290 mV vs Fc/Fc^+ in solution. The reversible oxidation behavior is maintained even when **5** was immobilized on the ITO electrode by photoinduced CROP. The oxidation potential is, however, more positive by 240 mV. This is consistent with an increased activation barrier for electron transfer owing to the insulating character of the

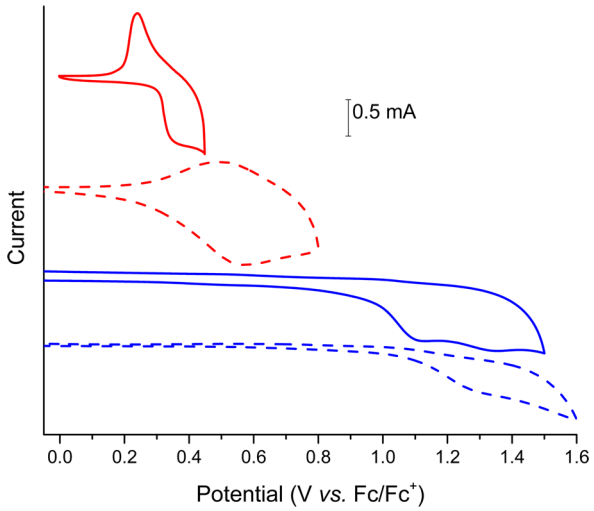

Figure 3. Anodic cyclic voltammograms of **4** (blue) and **5** (red) measured in 0.1 M $TBAPF_6$ dichloromethane (solid line) and immobilized on ITO-coated glass electrodes by photoinduced CROP (dashed line) in 0.1 M $TBAPF_6$ acetonitrile at a scan rate of 100 mV/s.

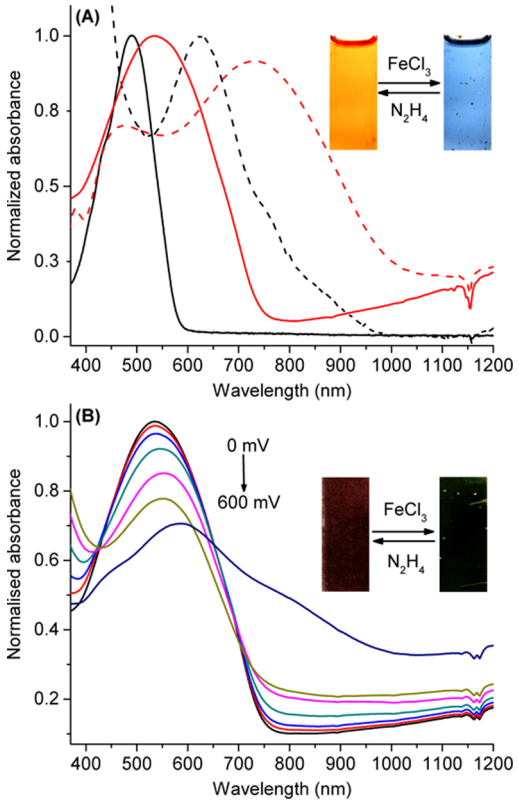

Figure 4. (A) Normalized absorbance spectra of **5** in dichloromethane (black line) and photopolymerized on ITO-glass (red line) in the neutral (solid line) and oxidized (dashed line) states with ferric chloride. Inset: pictures of the neutral **5** in solution and its oxidized (right) and neutralized (left) states obtained by adding hydrazine hydrate and ferric chloride, respectively. (B) Spectroelectrochemistry of the photopolymerized **5** on ITO by applying 0, 100, 200, 300, 400, 500, and 600 mV vs Fc/Fc^+ for given intervals. Inset: pictures of the photopolymerized **5** in the neutral (left) and oxidized (right) states obtained by chemical oxidation and neutralization.

film.[70,71] The oxidation potential of **4** was also increased by 280 mV when it was subjected to photoinduced CROP on the ITO electrode. In contrast to **5**, the oxidation of **4** was irreversible. The reversible behavior of **5** is courtesy of its terminal amines that prevent the electrochemically generated radical cation from reacting via cross-coupling routes. The oxidized intermediate of the immobilized layer was assigned to the radical cation according to the 59/n mV relationship for the forward and reverse peak separation.[71] Interestingly, the oxidation of **5** in solution was a two-electron process. While the identity of the intermediate cannot be unequivocally assigned to either a double radical cation or a dication, the terminal groups greatly affect the oxidation potential. The donating effect of the amine lowers the oxidation potential to potentials that are compatible for use in working devices, but are stable under aerobic conditions. Whereas, the electron withdrawing effect of the carbonyl in **4** increases the oxidation potential.

Detectable color change between the neutral and charged states of the photoinduced CROP layer in addition to reversible oxidation is paramount for using the polymer in electrochromic devices. Since reversible oxidation was confirmed (vide supra), the reversible color change of **5** in solution and immobilized on the substrate was examined. Chemical oxidation with ferric chloride was initially done to confirm the reversible visible color switching between the neutral and oxidized states. The neutral **5** changed from red to blue when oxidized (inset Figure 4A) in dichloromethane. The resulting observed absorbance for the neutral and oxidized states respectively was 492 and 628 nm. The oxidized state could be reduced to the neutral form with hydrazine hydrate. The absorbance of the neutral state obtained by reducing the oxidized state did not differ from the absorbance of the original neutral state. The persistent oxidized intermediate and reversible color change between the neutral and oxidized state demonstrate the robustness of the film and the azomethine bonds toward chemical doping. Furthermore, the reversibility of the doping process under ambient conditions implies that both the neutral and the oxidized states are stable. Similar chemically induced spectral changes were observed with **4**. A large red-shift of 66 nm was observed upon oxidizing **4**. While a larger red-shift was observed with **4**, the color switching perceived with the eye is not as interesting for commercial applications as that of the immobilized **5**. When immobilized on glass, the color of **5** was different from what was observed in solution (Figure 4A). The immobilized **5** was mauve in color, and it underwent a 198 nm bathochromic shift when chemically oxidized, resulting in visually green colored film (inset Figure 4B). The spectral differences observed between the solution and photopolymerized samples are most likely from intermolecular charge transfer and π-stacking in the thin films. Unlike what was observed in solution, the oxidized state of the immobilized **5** was not persistent. The chemically induced green color dissipated, and it was replaced with the original mauve color of the neutral state, immediately upon removing the substrate of **5** from the ferric chloride solution. The rapid color reversion is from evaporation of the solvent and self-quenching, but not from degradation of the azomethine. This was confirmed by regenerating the green doped state upon submerging the substrate in the oxidizing solution that led to similar absorbance spectra before and after doping. The corresponding CIE $L^*a^*b^*$ color coordinates of the different states are found in Table 1 and Supporting Information Figure S14.

The spectroelectrochemistry of **5** immobilized on a working ITO electrode was done to assess the color transition and

Table 1. CIE Coordinates with D65 illumination and 2° Observer Angle for the Different States of 5 in Solution and Photopolymerized on ITO Substrates

	state	L^*	a^*	b^*
solution	neutral[a]	88	20	24
	oxidized[a,b]	93	−1	6
	oxidized[c]	90	−7	6
immobilized	neutral[d]	44	18	−13
	oxidized[b,d]	56	3	−9
	oxidized[c]	66	−2	−2
electrochromic device	neutral[e]	80	13	1
	oxidized[b,e]	83	5	1

[a]**5** in acetonitrile with $TBAPF_6$ as the supporting electrolyte. [b]Electrochemically oxidized by applying a potential of 0.6 V vs Fc/Fc^+. [c]Chemically oxidized with ferric chloride in dichloromethane. [d]**5** immobilized on the ITO electrode measured in acetonitrile with $TBAPF_6$ as the supporting electrolyte. [e]Photopolymerized **5** used as the electrochromic layer in the working transmissive electrochromic device.

switching capacity of the polymer under conditions similar to those in a working electrochromic device. This study was also done to corroborate the chemical oxidation studies. For the spectroelectrochemical studies, the oxidation potential, reversible oxidation, color changes, and the oxidation/neutralization switching rates of the immobilized polymer were examined in acetonitrile using $TBAPF_6$ as the supporting electrolyte. The electrochemical oxidation of **5** led to stark color changes between its neutral and oxidized states (inset Figure 5B) with

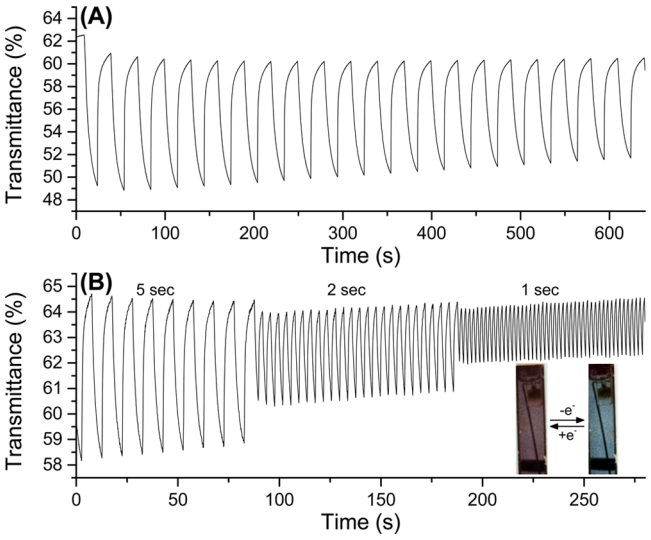

Figure 5. (A) Change in transmittance of **5** immobilized on ITO electrode measured at 15 s intervals and monitored at 810 nm. (B) Change in transmittance of **5** immobilized on ITO electrode measured at 5, 2, and 1 s intervals and monitored at 750 nm with potentials switched between +0.6 and −0.6 V vs Fc/Fc^+ in 0.1 M $TBAPF_6$ acetonitrile. Inset: photographs of the immobilized films of **5** on an ITO glass electrode in the neutral (left) and oxidized (right) states.

applied biases of +0.6 and −0.6 V vs Fc/Fc^+. Similar to the chemical doping studies, two distinct colors were observed by spectroelectrochemistry for the oxidized and neutral states. The observed color change was consistent with the chemically induced mauve-to-green color change. The CIE coordinates of the neutral and oxidized states were determined using the D65 illumination and 2° observer angle (Table 1). The electrochemical switching was done under ambient conditions without degassed or anhydrous solvents, demonstrating the stability of both the neutral and the oxidized states. The chemical and spectroelectrochemical studies additionally demonstrated that **5** had spectral and electrochemical properties that are suitable for its use as the electrochromic layer in devices. It is worthy to note that **5** is the first example of a polyazomethine prepared by photolithographic means that can be reversibly oxidized with significant color changes in the visible spectrum between its neutral and oxidized states. Films were also prepared from **4** using the same process. As expected, the oxidation of the polymer film was not reversible and the film rapidly degraded with multiple switching between the neutral and oxidized states (Supporting Information Figure S14), owing to electrochemically induced reactions at the unsubstituted thiophene positions.[52]

The capacity of the immobilized polymer to continuously switch between its neutral and oxidized states and its switching speed were investigated. These were done to further assess the stability and robustness of the immobilized electrochromic **5**. The duty cycle of the immobilized polymer was examined with 15 s switching speeds. This was found to be the optimal switching interval for the largest transmittance change between the neutral and oxidized states. As seen in Figure 5A, the immobilized polymer could be switched for many cycles without any significant variation in the transmittance. Switching between the two colored states of the photopolymerized **5** at various speeds was possible, as seen in Figure 5B. Increasing the switching from 15 to 1 s. led to a reduced transmittance difference between the neutral and oxidized states. To some extent, the slow switching speed is not surprising because of the slow diffusion of the large bulky $TBAPF_6$ electrolyte through the electrochromic layer and associated conformational changes of the polymer film.[72,73] Nonetheless, color changes were still visually observed even with switching speeds up to 1 s. The spectroelectrochemical data confirm that the azomethine bonds of **5** are robust and they can withstand repeated switching between their neutral and oxidation states under ambient conditions. While extended duty cycles are beneficial for device applications, the switching cycles observed in Figure 5 under simulated working device conditions nevertheless demonstrate that conventional photolithography can be used for immobilizing electroactive azomethines directly on electrodes. This proof-of-concept proves that immobilized azomethines are electroactive and they can sustain repeated cycling without color fatigue or decomposition. Meanwhile, preliminary results obtained with a standard unoptimized electrochromic device using photopolymerized **5** as the electrochromic layer demonstrate that the immobilized azomethine can be used as an alternative electrochrome to currently used materials (Supporting Information Figures S26 and S27). Extended duty cycles for end-user applications are expected with **5** upon improving film preparation, controlled film thickness, and optimization of supporting electrolytes.

CONCLUSION

In summary, the first example of an electrochromic azomethine consisting of an oxetane photopolymerizable group was reported. The first example of photopatterning an azomethine using standard photolithographic methods to yield a robust and immobilized polymer directly on the working transparent electrode was also reported. This polymerization method has

the advantage that electroactive materials ranging from micrometer to centimeter dimensions, and potentially nanometer scale, can be prepared while retaining the electroactive properties required for device usage. The material was found to have key properties including reversible oxidation, visible color switching between the neutral and the oxidized states, and stability toward repeated neutralization and oxidation cycles under ambient conditions. These properties are of importance considering that azomethines are often overlooked as functional materials. The photopolymerized layer served as a proof-of-concept that azomethines are viable electrochromic materials. Extended duty cycles of the photoimmobilized azomethines in a working electrochromic device are expected with optimized device fabrication, including appropriate electrolytes. The advantage of these materials is their potential application to large scale processing methods for patterning over a wide range of dimensions, while preserving their electrochromic properties.

EXPERIMENTAL SECTION

General Procedures. All chemicals and reagents were obtained from commercial sources, unless otherwise stated. Anhydrous and degassed solvents were obtained from an activated alumina solvent purification system.

Spectroscopy. Both solution and thin film absorbance measurements were done on a Cary 500 spectrophotometer. FT-IR measurements were done on a Thermo scientific spectrometer Nicolet 6700 FT-IR instrument with an ATR accessory. The photoactive mixture of **5** (vide infra) was deposited by drop-casting onto multiple glass slides. The slides were irradiated for prescribed times. The substrates were then rinsed to remove the unpolymerized **5** as below and then FT-IR measurements of the immobilized **5** were done.

Electrochemistry. Cyclic voltammetry measurements were made on a Bio-Logic VPS 300 potentiostat. Compounds were dissolved in degassed dichloromethane at 10^{-3} M with 0.1 M $TBAPF_6$. A platinum electrode was used as the working electrode with a platinum wire as the auxiliary electrode. An $Ag/AgNO_3$ (0.01 M in CH_3CN) electrode was used as a reference and checked against the ferrocene/ferrocenium couple (Fc/Fc^+). Ferrocene was added to the solution as an internal reference, and the potentials were reported relative to the Fc/Fc^+ couple.[74,75] The spectroelectrochemistry was done using a Pt wire mesh electrode as the working electrode. Ferrocene was also used as an internal reference, and all the potentials were reported with respect to the ferrocene/ferrocenium couple, unless otherwise stated.[74] Spectroelectrochemical measurements were done using the electrochemical method above by using a special 1 mm thick quartz absorbance cell. The working electrode was a 1 mm thick platinum mesh gauge electrode. Switching studies between the oxidized and neutral states were done by applying a potential 310 mV greater than the E_{ox} for the compound of study. The corresponding spectra were measured after applying a given potential for 30 s. Spectra at 810 nm, corresponding to the oxidized state, were continuously recorded while electrochemically switching between the neutral and the oxidized states.

Photolithography. In chloroform (0.5 mL) under ambient conditions were dissolved **5** (1.6 mg), the photoacid generator *p*-octyloxy-phenyl-phenyl iodonium hexafluoroantimonate (OPPI; Spectra Group, Inc.; 2 mg), 5,7-diiodo-3-butoxy-6-fluorone (H-Nu-470; Spectra Group, Inc.; 1 mg) as the photosensitizer, and 9,10-diethoxyanthracene (AN-910-E; Spectra Group, Inc.; 1.2 mg) as the electron transfer accelerator.[76] Optimization of the photolithographic solutions was done by drop-casting the solutions onto glass substrates. The resulting film was placed in a photoreactor and irradiated at 350 nm for 10 min (247.5 $Lm{\cdot}m^{-2}$). The substrate was then baked in an oven at 100 °C for 60 min. The unpolymerized **5** was subsequently removed by washing the substrate with a mixture of dichloromethane/triethylamine (8/2) and then neat dichloromethane. The photolithographic steps including irradiation, baking, and rinsing were all done under ambient conditions. Photopolymerized films of sufficient thickness for optical and spectroelectrochemical measurements were obtained by spray-coating the optimized solution of **5** as per above.

The same photolithographic procedure was used for electrochemical measurements. The samples were spray-coated onto ITO coated glass substrates (Delta Technologies, Inc.) Photopatterning was done by placing a mask having the desired pattern over the spin-coated film prior to irradiation. The mask was removed after irradiating the substrate and prior to baking.

The thickness and roughness and the resulting photopolymerized films were determined using a stylus Dektak profilometer (Bruker, Nanoscience). The photopatterns were characterized and images photographed using an Axioskop-40 microscope from Carl Zeiss, equipped with 10 and 20 objectives. Pictures were taken with a Micropublisher 3.3 camera from Q-Imaging and analyzed with the Image-Pro Plus 5.1 software.

Electrochromic devices were prepared by spray-coating a solution of **5** onto ITO coated glass. For this, **5** (10 mg) was dissolved in dichloromethane (1 mL) along with OPPI (6 mg), H-Nu-470 (3 mg), and AN-910-E (3.6 mg). The film coated substrate was placed in a photoreactor, and it was irradiated at 350 nm for 10 min. The substrate was then baked in an oven at 100 °C for 60 min. The unpolymerized **5** was subsequently washed with a mixture of dichloromethane/triethylamine (8/2 vol %) and then neat dichloromethane. The electrolyte gel was prepared by combining propylene carbonate (PC), poly(ethylene glycol) diacrylate, and tetrabutylammonium tetrafluoroborate in the respective weight ratios of 10:7:3. 2,2-Dimethoxy-2-hexylacetophenone was used as the photoinitiator, which was added to the gel mixture in a 17.5 mg to 5 g ratio to PC. The gel was deposited with a Pasteur pipet on the ITO substrate, and the film of **5** was placed on the top of the gel. The device was irradiated at 350 nm during 5 min to cross-link the gel. Copper tape was used for electrical contacts, and the spectroelectrochemical properties were measured as above.

Synthesis. *2-(2,5-Dibromo-3-thienyl)ethanol (**1**).*[77] In the absence of light, a solution of NBS (15.23 g, 85.56 mmol) in DMF (60 mL) was added dropwise to a solution of 3-thiophene ethanol (4.76 g, 37.13 mmol) in DMF (90 mL) at room temperature and the reaction was stirred during 2.5 h at 40 °C and then 12 h at room temperature. The product was extracted with dichloromethane (150 mL), and the resulting organic layer was washed with water (5 × 250 mL), dried over $MgSO_4$, filtered, and concentrated to dryness. The product was purified by column chromatography on silica gel (eluent: dichloromethane) to give a colorless oil (9.90 g, 93% yield). ^{1}H NMR (400 MHz, $CDCl_3$) δ: 6.88 (s, 1H), 3.82 (t, 2H, ^3J = 6.5 Hz), 2.81 (t, 2H, ^3J = 6.5 Hz), 1.44 (s, 1H). ^{13}C (100 MHz, $CDCl_3$) δ: 139.5, 131.7, 111.2, 109.8, 62.2, 33.2. HR-MS (ESI) (M + H) *m*/*z*: calcd for $C_6H_7Br_2OS$, 284.8571; found, 284.8579.

*3-((2-(2,5-Dibromothiophen-3-yl)ethoxy)methyl)-3-methyloxetane (**2**).* **1** (1.50 g, 5.24 mmol) and (3-methyloxetan-3-yl)methyl 4-methylbenzenesulfonate (1.60 g, 6.24 mmol) were dissolved in THF (120 mL) along with KOH (1.17 g, 20.85 mmol). The solution was stirred at reflux during 72 h. Afterward the solvent was evaporated and the residue was dissolved in dichloromethane (300 mL). The organic layer was washed with water (3 × 150 mL), dried over $MgSO_4$, filtered, and concentrated to dryness. The product was purified by column chromatography on silica gel (eluent: 1/1 hexane/diethyl ether) to give a colorless oil (1.40 g, 72% yield). ^{1}H NMR (400 MHz, $CDCl_3$) δ: 6.86 (s, 1H), 4.48 (d, 2H, ^2J = 5.7 Hz), 4.35 (d, 2H, ^2J = 5.7 Hz), 3.62 (t, 2H, ^3J = 6.5 Hz), 3.49 (s, 2H), 2.81 (t, 2H, ^3J = 6.5 Hz), 1.30 (s, 3H). ^{13}C (100 MHz, $CDCl_3$) δ: 140.0, 131.9, 110.7, 109.4, 80.4, 70.6, 40.3, 30.3, 21.7. HR-MS (ESI) (M + H) *m*/*z*: calcd for $C_{11}H_{15}Br_2O_2S$, 368.9149; found, 368.9154.

*(3-(2-((3-Methyloxetan-3-yl)methoxy)ethyl)thiophene-2,5-diyl)-bis(tributylstannane) (**3**).* Under nitrogen, a solution of 1.6 M *n*-BuLi in hexane (1.25 mL, 2.00 mmol) was added dropwise to a solution of **2** (200 mg, 0.54 mmol) in anhydrous THF (14 mL), and then it was cooled to −78 °C. After stirring for 1 h at −78 °C, Bu_3SnCl (0.41 mL, 1.50 mmol) was slowly added. The reaction mixture was allowed to reach room temperature. After addition of diethyl ether (100 mL), the mixture was washed with a saturated aqueous solution of NH_4Cl (200

mL), dried over $MgSO_4$, and concentrated to dryness to give a light yellow oil corresponding to **3**. The crude product was immediately used in the Stille coupling reaction without further purification.

*3′-(2-((3-Methyloxetan-3-yl)methoxy)ethyl)-[2,2′:5′,2″-terthiophene]-5,5″-dicarbaldehyde (**4**).* A mixture **3** and 5-bromo-2-thiophene carboxaldehyde (0.13 mL, 1.10 mmol) in toluene (5 mL) was degassed with argon for 20 min in a Schlenk flask. After adding $Pd(PPh_3)_4$ (60 mg, 0.05 mmol), the Schlenk flask was closed and the reaction mixture was stirred at 110 °C for 12 h. After removing the solvent by evaporation in vacuo, the residue was purified by chromatography on silica gel (eluent: 9/1 dichloromethane/acetone) to give **4** (110 mg, two-steps 47% yield) as a yellow oil. ^{1}H NMR (400 MHz, $CDCl_3$) δ: 9.90 (s, 1H), 9.87 (s, 1H), 7.73 (d, 1H, ^3J = 4.0 Hz), 7.68 (d, 1H, ^3J = 4.0 Hz), 7.32 (d, 1H, ^3J = 3.9 Hz), 7.32 (s, 1H), 7.27 (d, 1H, ^3J = 3.9 Hz), 4.47 (d, 2H, ^2J = 5.7 Hz), 4.33 (d, 2H, ^2J = 5.7 Hz), 3.77 (t, 2H, ^3J = 6.2 Hz), 3.51 (s, 2H), 3.10 (t, 2H, ^3J = 6.2 Hz), 1.28 (s, 3H). ^{13}C NMR (100 MHz, $CDCl_3$) δ: 182.7, 182.6, 146.0, 144.8, 143.3, 142.4, 139.7, 137.4, 136.9, 135.7, 132.3, 129.9, 127.3, 124.9, 80.1, 76.5, 70.8, 40.0, 30.1, 21.5. HR-MS (ESI) (M + H) *m/z*: calcd for $C_{21}H_{21}O_4S_3$, 433.0592; found, 433.0597.

*Tetraethyl 5,5′-((1E,1′E)-((3′-(2-((3-Methyloxetan-3-yl)methoxy)-ethyl)-[2,2′:5′,2″-terthiophene]-5,5″-diyl)bis(methanylylidene))bis-(azanylylidene))bis(2-aminothiophene-3,4-dicarboxylate) (**5**).* Scandium triflate (5 mg, 0.01 mmol) was added to a mixture of **4** (240 mg, 0.55 mmol) and **6** (285 mg, 1.10 mmol) in ethanol (40 mL). The reaction mixture was refluxed for 2 h. The solvent was then evaporated under vacuum. The resulting crude product was dissolved in acetone, and it was precipitated by adding hexane. The crude product was filtered, and it was purified by column chromatography on silica gel (eluent: 8/2 hexane/acetone) to give **5** (380 mg, 76% yield) as a red powder. ^{1}H NMR (400 MHz, acetone) δ: 8.21 (s, 1H), 8.19 (s, 1H), 7.52 (s, 4H), 7.51 (d, 1H, ^3J = 4.0 Hz), 7.46 (d, 1H, ^3J = 3.9 Hz), 7.42 (s, 1H), 7.34 (d, 1H, ^3J = 3.9 Hz), 7.32 (d, 1H, ^3J = 3.9 Hz), 4.42 (d, 2H, ^2J = 5.6 Hz), 4.40–4.33 (m, 4H), 4.25–4.17 (m, 6H), 3.84 (t, 2H, ^3J = 6.3 Hz), 3.56 (s, 2H), 3.13 (t, 2H, ^3J = 6.3 Hz), 1.44–1.38 (m, 6H), 1.30–1.25 (m, 9H). ^{13}C NMR (100 MHz, $CDCl_3$) δ: 165.5, 164.8, 161.8, 145.9, 145.9, 143.7, 142.8, 141.1, 140.0, 139.6, 136.1, 133.6, 133.4, 133.4, 133.1, 132.4, 131.4, 131.3, 129.7, 128.1, 125.8, 102.5, 79.9, 76.9, 71.4, 61.6, 61.6, 60.5, 40.6, 21.7, 14.9, 14.8, 14.6, 14.5. HR-MS (ESI) (M + H) *m/z*: calcd for $C_{41}H_{45}N_4O_{10}S_5$, 913.1723; found, 913.1734.

■ ASSOCIATED CONTENT

Ⓢ Supporting Information

Absorbance, ATR-FTIR, and NMR spectra, cyclic voltammograms, and photographs showing the reversible color changes. This material is available free of charge via the Internet at http://pubs.acs.org.

■ AUTHOR INFORMATION

Corresponding Author

*E-mail: w.skene@umontreal.ca.

Present Address

†Institute of Chemical and Engineering Sciences, 1 Pesek Road, Jurong Island, Singapore 627833, Singapore (S.B.).

Notes

The authors declare no competing financial interest.

■ ACKNOWLEDGMENTS

Financial support from the Natural Sciences and Engineering Research Council of Canada is acknowledged for Discovery, Strategic Research, I2I, and Research Tools and Instrument grants. Canadian Foundation for Innovation is also acknowledged for additional equipment and infrastructures. The Center for Self-Assembled Chemical Structures is also acknowledged. Mr. Pierre Menard-Tremblay is additionally thanked for assistance with the microscope images. Mr. Alireza Mesgar's assistance with the photopatterning is also acknowledged.

■ REFERENCES

(1) Monk, P. M. S.; Mortimer, R. J.; Rosseinsky, D. R. *Electrochromism and Electrochromic Devices*; Cambridge University Press: Cambridge, 2007.

(2) Thakur, V. K.; Ding, G.; Ma, J.; Lee, P. S.; Lu, X. Hybrid Materials and Polymer Electrolytes for Electrochromic Device Applications. *Adv. Mater.* **2012**, *24*, 4071–96.

(3) Zilberberg, K.; Meyer, J.; Riedl, T. Solution Processed Metal-Oxides for Organic Electronic Devices. *J. Mater. Chem. C* **2013**, *1*, 4071–4096.

(4) Zhao-Yang, Z.; Yi-Jie, T.; Xiao-Qian, X.; Yong-Jiang, Z.; Hai-Feng, C.; Wen-Wei, Z. Multicolor Electrochromism of Low-Bandgap Copolymers Based on Pyrrole and 3,4-Ethylenedioxythiophene: Fine-Tuning Colors Through Feed Ratio. *J. Appl. Polym. Sci.* **2013**, *129*, 1506–1512.

(5) Ma, L.; Zhao, P.; Wu, W.; Niu, H.; Cai, J.; Lian, Y.; Bai, X.; Wang, W. Functioned RGO with PolySchiff Base: Sensor for TNT, Acidochromic and Electrochromic Multi-Properties. *Polym. Chem.* **2013**, *4*, 4746–4754.

(6) Lee, K.-R.; Sotzing, G. A. Green and Blue Electrochromic Polymers from Processable Siloxane Precursors. *Chem. Mater.* **2013**, *25*, 2898–2904.

(7) Xu, C.; Zhao, J.; Cui, C.; Wang, M.; Kong, Y.; Zhang, X. Triphenylamine-Based Multielectrochromic Material and Its Neutral Green Electrochromic Devices. *J. Electroanal. Chem.* **2012**, *682*, 29–36.

(8) Bhuvana, T.; Kim, B.; Yang, X.; Shin, H.; Kim, E. Reversible Full-Color Generation with Patterned Yellow Electrochromic Polymers. *Angew. Chem., Int. Ed.* **2013**, *52*, 1180–1184.

(9) Sassi, M.; Salamone, M. M.; Ruffo, R.; Mari, C. M.; Pagani, G. A.; Beverina, L. Gray to Colorless Switching, Crosslinked Electrochromic Polymers with Outstanding Stability and Transmissivity from Naphthalenediimmide-Functionalized EDOT. *Adv. Mater.* **2012**, *24*, 2004–2008.

(10) Mei, J.; Heston, N. C.; Vasilyeva, S. V.; Reynolds, J. R. A Facile Approach to Defect-Free Vinylene-Linked Benzothiadiazole-Thiophene Low-Bandgap Conjugated Polymers for Organic Electronics. *Macromolecules* **2009**, *42*, 1482–1487.

(11) Beaujuge, P. M.; Vasilyeva, S. V.; Ellinger, S.; McCarley, T. D.; Reynolds, J. R. Unsaturated Linkages in Dioxythiophene-Benzothiadiazole Donor-Acceptor Electrochromic Polymers: The Key Role of Conformational Freedom. *Macromolecules* **2009**, *42*, 3694–3706.

(12) Yu, N.; Zhu, R.; Peng, B.; Huang, W.; Wei, W. Synthesis and Characterization of Poly(Fluorene Vinylene) Copolymers Containing Thienylene-Vinylene Units. *J. Appl. Polym. Sci.* **2008**, *108*, 2438–2445.

(13) Morin, J.-F.; Drolet, N.; Tao, Y.; Leclerc, M. Syntheses and Characterization of Electroactive and Photoactive 2,7-Carbazolenevinylene-Based Conjugated Oligomers and Polymer. *Chem. Mater.* **2004**, *16*, 4619–4626.

(14) Yen, H.-J.; Chen, C.-J.; Liou, G.-S. Flexible Multi-Colored Electrochromic and Volatile Polymer Memory Devices Derived from Starburst Triarylamine-Based Electroactive Polyimide. *Adv. Funct. Mater.* **2013**, *23*, 5307–5316.

(15) Xu, J.; Neo, W. T.; Wang, X.; Cho, C. M.; Song, J.; Chan, H. S. O.; Zong, Y.; Loo, L. M. Solution-Processable Blue-to-Transmissive Electrochromic Benzotriazole-Containing Conjugated Polymers. *Polym. Chem.* **2013**, *4*, 4663–4675.

(16) Shi, P.; Amb, C. M.; Dyer, A. L.; Reynolds, J. R. Fast Switching Water Processable Electrochromic Polymers. *ACS Appl. Mater. Interfaces* **2012**, *4*, 6512–6521.

(17) Chen, F.; Fu, X.; Zhang, J.; Wan, X. Near-Infrared and Multicolored Electrochromism of Solution Processable Triphenylamine-Anthraquinone Imide Hybrid Systems. *Electrochim. Acta* **2013**, *99*, 211–218.

(18) Hu, B.; Lv, X.; Sun, J.; Bian, G.; Ouyang, M.; Fu, Z.; Wang, P.; Zhang, C. Effects on the Electrochemical and Electrochromic Properties of 3,6 Linked Polycarbazole Derivative by The Introduction

of Different Acceptor Groups and Copolymerization. *Org. Electron.* **2013**, *14*, 1521−1530.
(19) Cai, J.; Zhao, P.; Niu, H.; Lian, Y.; Wang, C.; Bai, X.; Wang, W. Reducing Polyazomethine to Poly(N-Phenylbenzylamine) with Near Infrared Electrochromic, Fluorescence and Photovoltaic Properties. *Polym. Chem.* **2013**, *4*, 1183−1192.
(20) Yen, H.-J.; Liou, G.-S. Solution-Processable Triarylamine-Based Electroactive High Performance Polymers for Anodically Electrochromic Applications. *Polym. Chem.* **2012**, *3*, 255−264.
(21) Akpinar, H. Z.; Udum, Y. A.; Toppare, L. Spray-Processable Thiazolothiazole-Based Copolymers with Altered Donor Groups and Their Electrochromic Properties. *J. Polym. Sci., Part A: Polym. Chem.* **2013**, *51*, 3901−3906.
(22) Reeves, B. D.; Unur, E.; Ananthakrishnan, N.; Reynolds, J. R. Defunctionalization of Ester-Substituted Electrochromic Dioxythiophene Polymers. *Macromolecules* **2007**, *40*, 5344−5352.
(23) Amb, C. M.; Beaujuge, P. M.; Reynolds, J. R. Spray-Processable Blue-to-Highly Transmissive Switching Polymer Electrochromes via the Donor-Acceptor Approach. *Adv. Mater.* **2010**, *22*, 724−728.
(24) Smith, Z. C.; Pawle, R. H.; Thomas, S. W. Photoinduced Aggregation of Polythiophenes. *ACS Macro Lett.* **2012**, 825−829.
(25) Helgesen, M.; Bjerring, M.; Nielsen, N. C.; Krebs, F. C. Influence of the Annealing Temperature on the Photovoltaic Performance and Film Morphology Applying Novel Thermocleavable Materials. *Chem. Mater.* **2010**, *22*, 5617−5624.
(26) Kim, B. J.; Miyamoto, Y.; Ma, B.; Fréchet, J. M. J. Photocrosslinkable Polythiophenes for Efficient, Thermally Stable, Organic Photovoltaics. *Adv. Funct. Mater.* **2009**, *19*, 2273−2281.
(27) Akimoto, S.; Kato, D.; Jikei, M.; Kakimoto, M.-a. A Novel Main Chain Cleavable Photosensitive Polyimide: Polyimide Containing Acetal Structure with Photoacid Generator. *J. Photopolym. Sci. Technol.* **1999**, *12*, 245−248.
(28) Burdi, D.; Hoyt, S.; Begley, T. P. Design of a Cleavable Linker for the Synthesis of a C*is-Syn* Pyrimidine Photodimer. *Tetrahedron Lett.* **1992**, *33*, 2133−2136.
(29) Dyer, A. L.; Thompson, E. J.; Reynolds, J. R. Completing the Color Palette with Spray-Processable Polymer Electrochromics. *ACS Appl. Mater. Interfaces* **2011**, *3*, 1787−1795.
(30) Bokria, J. G.; Kumar, A.; Seshadri, V.; Tran, A.; Sotzing, G. A. Solid-State Conversion of Processable 3,4-Ethylenedioxythiophene (EDOT) Containing Poly(Arylsilane) Precursors to π-Conjugated Conducting Polymers. *Adv. Mater.* **2008**, *20*, 1175−1178.
(31) Sicard, L.; Navarathne, D.; Skalski, T.; Skene, W. G. On-Substrate Preparation of An Electroactive Conjugated Polyazomethine from Solution Processable Monomers and Its Application in Electrochromic Devices. *Adv. Funct. Mater.* **2013**, *23*, 3549−3559.
(32) Alkan, S.; Cutler, C. A.; Reynolds, J. R. High-Quality Electrochromic Polythiophenes via $BF_3{\cdot}Et_2O$ Electropolymerization. *Adv. Funct. Mater.* **2003**, *13*, 331−336.
(33) Ding, Y.; Invernale, M. A.; Mamangun, D. M. D.; Kumar, A.; Sotzing, G. A. A simple, low waste and versatile procedure to make polymer electrochromic devices. *J. Mater. Chem.* **2011**, *21*, 11873−11878.
(34) Bolduc, A.; Skene, W. G. Direct Preparation of Electroactive Polymers on Electrodes and Their Use in Electrochromic Devices. *Polym. Chem.* **2014**, *5*, 1119−1123.
(35) Navarathne, D.; Skene, W. G. Dynachromes-Dynamic Electrochromic Polymers Capable of Property Tuning and Patterning via Multiple Constitution Component Exchange. *J. Mater. Chem. C* **2013**, *41*, 6743−6747.
(36) Crivello, J. V.; Falk, B.; Zonca, M. R. Photoinduced Cationic Ring-Opening Frontal Polymerizations of Oxetanes and Oxiranes. *J. Polym. Sci., Part A: Polym. Chem.* **2004**, *42*, 1630−1646.
(37) Zuniga, C. A.; Abdallah, J.; Haske, W.; Zhang, Y.; Coropceanu, I.; Barlow, S.; Kippelen, B.; Marder, S. R. Crosslinking Using Rapid Thermal Processing for the Fabrication of Efficient Solution-Processed Phosphorescent Organic Light-Emitting Diodes. *Adv. Mater.* **2013**, *25*, 1739−1744.
(38) Feser, S.; Meerholz, K. Investigation of the Photocross-Linking Mechanism in Oxetane-Functionalized Semiconductors. *Chem. Mater.* **2011**, *23*, 5001−5005.
(39) Charas, A.; Morgado, J. Oxetane-Functionalized Conjugated Polymers in Organic (Opto)Electronic Devices. *Curr. Phys. Chem.* **2012**, *2*, 241−264.
(40) Kulshreshtha, P. K.; Maruyama, K.; Kiani, S.; Dhuey, S.; Perera, P.; Blackwell, J.; Olynick, D.; Ashby, P. D. Sub-20nm Lithography Negative Tone Chemically Amplified Resists Using Cross-Linker Additives. *Proc. SPIE* **2013**, *8682*, 86820N−86820N-10.
(41) Yang, C.-J.; Jenekhe, S. A. Conjugated Aromatic Poly(Azomethines). 1. Characterization of Structure, Electronic Spectra, and Processing of Thin Films from Soluble Complexes. *Chem. Mater.* **1991**, *3*, 878−887.
(42) Bolduc, A.; Al Ouahabi, A.; Mallet, C.; Skene, W. G. Insight into the Isoelectronic Character of Azomethines and Vinylenes Using Representative Models: A Spectroscopic and Electrochemical Study. *J. Org. Chem.* **2013**, *78*, 9258−9269.
(43) Navarathne, D.; Skene, W. G. Towards Electrochromic Devices Having Visible Color Switching Using Electronic *Push-Push* And *Push-Pull* Cinnamaldehyde Derivatives. *ACS Appl. Mater. Interfaces* **2013**, *5*, 12646−12653.
(44) Barik, S.; Navarathne, D.; Leborgne, M.; Skene, W. G. Conjugated Thiophenoazomethines: Electrochromic Materials Exhibiting Visible-to-Near-IR Color Changes. *J. Mater. Chem. C* **2013**, *1*, 5508−5519.
(45) Park, J. Y.; Lee, J.; Kim, J.-B. Photo-Patternable Electroluminescent Blends of Polyfluorene Derivatives and Charge-Transporting Molecules. *Eur. Polym. J.* **2008**, *44*, 3981−3986.
(46) Rudati, P. S.; Mueller, D. C.; Meerholz, K. Preparation of Insoluble Hole-Injection Layers by Cationic Ring-Opening Polymerisation of Oxetane-Derivatized Triphenylamine Dimer for Organic Electronics Devices. *Proc. Chem.* **2012**, *4*, 216−223.
(47) Köhnen, A.; Riegel, N.; Müller, D. C.; Meerholz, K. Surface-Initiated Phase Separation−Fabrication of Two-Layer Organic Light-Emitting Devices in a Single Processing Step. *Adv. Mater.* **2011**, *23*, 4301−4305.
(48) Bayerl, M. S.; Braig, T.; Nuyken, O.; Müller, D. C.; Groß, M.; Meerholz, K. Crosslinkable Hole-Transport Materials for Preparation of Multilayer Organic Light Emitting Devices by Spin-Coating. *Macromol. Rapid Commun.* **1999**, *20*, 224−228.
(49) Jensen, J.; Dyer, A. L.; Shen, D. E.; Krebs, F. C.; Reynolds, J. R. Direct Photopatterning of Electrochromic Polymers. *Adv. Funct. Mater.* **2013**, *23*, 3728−3737.
(50) Amb, C. M.; Dyer, A. L.; Reynolds, J. R. Navigating the Color Palette of Solution-Processable Electrochromic Polymers. *Chem. Mater.* **2010**, *23*, 397−415.
(51) Argun, A. A.; Reynolds, J. R. Line patterning for Flexible and Laterally Configured Electrochromic Devices. *J. Mater. Chem.* **2005**, *15*, 1793−1800.
(52) Roncali, J. Conjugated Poly(Thiophenes): Synthesis, Functionalization, and Applications. *Chem. Rev.* **1992**, *92*, 711−738.
(53) Beaujuge, P. M.; Reynolds, J. R. Color Control in π-Conjugated Organic Polymers for Use in Electrochromic Devices. *Chem. Rev.* **2010**, *110*, 268−320.
(54) Gather, M. C.; Köhnen, A.; Falcou, A.; Becker, H.; Meerholz, K. Solution-Processed Full-Color Polymer Organic Light-Emitting Diode Displays Fabricated by Direct Photolithography. *Adv. Funct. Mater.* **2007**, *17*, 191−200.
(55) Giuseppone, N.; Schmitt, J.-L.; Schwartz, E.; Lehn, J.-M. Scandium(III) Catalysis of Transimination Reactions. Independent and Constitutionally Coupled Reversible Processes. *J. Am. Chem. Soc.* **2005**, *127*, 5528−5539.
(56) Giuseppone, N.; Schmitt, J.-L.; Lehn, J.-M. Generation of Dynamic Constitutional Diversity and Driven Evolution in Helical Molecular Strands under Lewis Acid Catalyzed Component Exchange. *Angew. Chem., Int. .Ed.* **2004**, *43*, 4902−4906.
(57) Hartwig, A.; Harder, A.; Lühring, A.; Schröder, H. (9-Oxo-9H-Fluoren-2-yl)-Phenyl-Iodonium Hexafluoroantimonate(V) - A Photo-

initiator for the Cationic Polymerisation of Epoxides. *Eur. Polym. J.* **2001**, *37*, 1449−1455.
(58) Crivello, J. V.; Lee, J. L. Alkoxy-Substituted Diaryliodonium Salt Cationic Photoinitiators. *J. Polym. Sci., Part A: Polym. Chem.* **1989**, *27*, 3951−3968.
(59) Reichmanis, E.; Houlihan, F. M.; Nalamasu, O.; Neenan, T. X. Chemical Amplification Mechanisms for Microlithography. *Chem. Mater.* **1991**, *3*, 394−407.
(60) Pérez Guarìn, S. A.; Bourgeaux, M.; Dufresne, S.; Skene, W. G. Photophysical, Crystallographic, and Electrochemical Characterization of Symmetric and Unsymmetric Self-Assembled Conjugated Thiopheno Azomethines. *J. Org. Chem.* **2007**, *72*, 2631−2643.
(61) Dufresne, S.; Skene, W. G. Unsymmetric Pyrrole, Thiophene, and Furan-Conjugated Comonomers Prepared Using Azomethine Connections: Potential New Monomers for Alternating Homocoupled Products. *J. Org. Chem.* **2008**, *73*, 3859−3866.
(62) Seixas de Melo, J.; Burrows, H. D.; Svensson, M.; Andersson, M. R.; Monkman, A. P. Photophysics of Thiophene Based Polymers in Solution: The Role of Nonradiative Decay Processes. *J. Chem. Phys.* **2003**, *118*, 1550−1556.
(63) Seixas de Melo, J.; Silva, L. M.; Arnaut, L. G.; Becker, R. S. Singlet and Triplet Energies of α-Oligothiophenes: A Spectroscopic, Theoretical, and Photoacoustic Study: Extrapolation to Polythiophene. *J. Chem. Phys.* **1999**, *111*, 5427−5433.
(64) Becker, R. S.; Seixas de Melo, J.; Maçanita, A. L.; Elisei, F. Comprehensive Evaluation of the Absorption, Photophysical, Energy Transfer, Structural, and Theoretical Properties of r-Oligothiophenes with One to Seven Rings. *J. Phys. Chem.* **1996**, *100*, 18683−18695.
(65) Muller, C. D.; Falcou, A.; Reckefuss, N.; Rojahn, M.; Wiederhirn, V.; Rudati, P.; Frohne, H.; Nuyken, O.; Becker, H.; Meerholz, K. Multi-Colour Organic Light-Emitting Displays by Solution Processing. *Nature* **2003**, *421*, 829−833.
(66) Köhnen, A.; Brücher, M.; Reckmann, A.; Klesper, H.; von Bohlen, A.; Wagner, R.; Herdt, A.; Lützenkirchen-Hecht, D.; Hergenröder, R.; Meerholz, K. Tracing a Moving Thin-Film Reaction Front with Nanometer Resolution. *Macromolecules* **2012**, *45*, 3487−3495.
(67) Lin, Y.; Zeng-Guo, F.; Yu-Mei, Z.; Feng, W.; Shi, C.; Guo-Qing, W. Synthesis and Application as Polymer Electrolyte of Hyperbranched Polyether Made by Cationic Ring-Opening Polymerization of 3-{2-[2-(2-Hydroxyethoxy)Ethoxy]Ethoxymethyl}-3′-Methyl-Oxetane. *J. Polym. Sci., Part A: Polym. Chem.* **2006**, *44*, 3650−3665.
(68) Li, C.; Shi, G. Polythiophene-Based Optical Sensors for Small Molecules. *ACS Appl. Mater. Interfaces* **2013**, *5*, 4503−4510.
(69) Li, Y. Molecular Design of Photovoltaic Materials for Polymer Solar Cells: Toward Suitable Electronic Energy Levels and Broad Absorption. *Acc. Chem. Res.* **2012**, *45*, 723−733.
(70) Settle, F. A. In *Handbook of Instrumental Techniques for Analytical Chemistry*; Settle, F. A., Ed.; Prentice Hall PTR: Upper Saddle River, NJ, 1997; pp 709−725.
(71) Bard, A. J.; Faulkner, L. R. *Electrochemical Methods: Fundamentals and Applications*, 2nd ed.; John Wiley & Sons: 2001.
(72) Otero, T. F.; Grande, H.-J.; Rodríguez, J. Reinterpretation of Polypyrrole Electrochemistry after Consideration of Conformational Relaxation Processes. *J. Phys. Chem. B* **1997**, *101*, 3688−3697.
(73) Otero, T. F.; Bengoechea, M. UV−Visible Spectroelectrochemistry of Conducting Polymers. Energy Linked to Conformational Changes. *Langmuir* **1999**, *15*, 1323−1327.
(74) Connelly, N. G.; Geiger, W. E. Chemical Redox Agents for Organometallic Chemistry. *Chem. Rev.* **1996**, *96*, 877−910.
(75) Tsierkezos, N. Cyclic Voltammetric Studies of Ferrocene in Nonaqueous Solvents in the Temperature Range from 248.15 to 298.15 K. *J. Solution Chem.* **2007**, *36*, 289−302.
(76) Zheldakov, I. L.; Grinevich, O.; Mejiritski, A.; Elles, C. G.; Neckers, D. C. Transient Spectroscopy of 5,7-Diiodo-3-Butoxy-6-Fluorone (DIBF). *Photochem. Photobiol.* **2014**, *90*, 335−337.
(77) Higgins, S. J.; Pounds, T. J.; Christensen, P. A. Syntheses and Electro(Co)Polymerization of Novel Thiophene- and 2,2′:5′,2″-Terthiophene-Functionalized Metal-Tetraazamacrocycle Complexes, and Electrochemical and Spectroelectrochemical Characterization of the Resulting Polythiophenes. *J. Mater. Chem.* **2001**, *11*, 2253−2261.
(78) Negoro, N.; Sasaki, S.; Mikami, S.; Ito, M.; Tsujihata, Y.; Ito, R.; Suzuki, M.; Takeuchi, K.; Suzuki, N.; Miyazaki, J.; Santou, T .; Odani, T.; Kanzaki, N.; Funami, M.; Morohashi, A.; Nonaka, M.; Matsunaga, S.; Yasuma, T.; Momose, Y. . Optimization of (2,3-Dihydro-1-benzofuran-3-yl)acetic Acids: Discovery of a Non-Free Fatty Acid-Like, Highly Bioavailable G Protein-Coupled Receptor 40/Free Fatty Acid Receptor 1 Agonist as a Glucose-Dependent Insulinotropic Agent. *J. Med. Chem.* **2012**, *55*, 3960−3974.